Kidney, Prostate, Testicle, and Uterus of Subjects Studied by MRS

Michael W. Weiner

University of California, San Francisco, CA, USA

1 KIDNEY

1.1 Proton MRS of Kidney

Shah et al.[1] reported a technique for using the stimulated echo amplitude mode (STEAM) sequence for ^{1}H MRS of the human kidney. The results demonstrated the presence of trimethylamines (TMAs). A prominent peak observed at 5.8 ppm was from urea. Avision et al.[2] used volume localized ^{1}H MRS to detect and measure changes in medullary trimethylamines in the human kidney (Figure 1). Proton magnetic resonance spectra were obtained from the human renal medulla using a stimulated echo localization sequence.

In addition to residual water and lipid, TMAs were identified at 3.25 ppm. In normal volunteers, overnight dehydration led to a significant increase of urine osmolality, and an increase in medullary TMAs (Figure 2). Water loading caused a water diuresis and a significant reduction in medullary TMAs within 4 hours. These results are consistent with the view that TMAs may play an osmoregulatory role in the medulla of the normal human kidney.

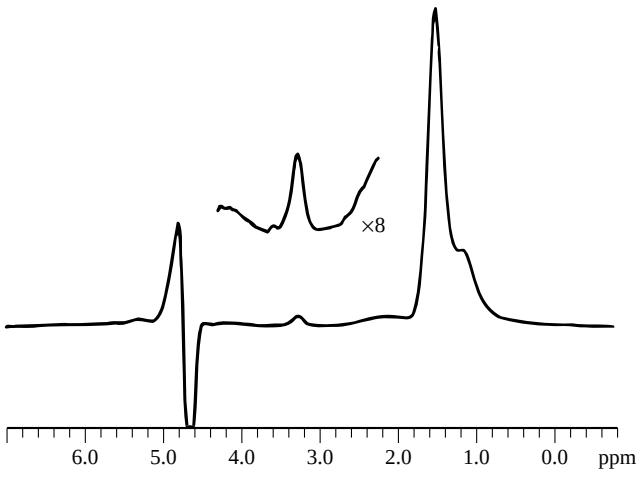

Figure 1 Water suppressed, volume localized ^{1}H spectrum from kidney. Water suppression consisted of a Silver–Hoult phase swept adiabatic fast passage pulse for selective water inversion followed by an inversion–recovery time of 0.8 second to allow the water Z magnetization to null. This sequence was delivered at the start of the volume localized stimulated echo sequence. TE = 68 ms, TM = 44 ms, TR = 3 s. Number of scans = 128. Filtering was 5 Hz of exponential line broadening. The resonances are water (4.75 ppm), lipids (0.9–1.4 ppm), and TMA (3.25 ppm)—which is shown expanded (×8) above the main spectrum. (Reproduced by permission of the National Academy of Sciences from Avison et al.[2])

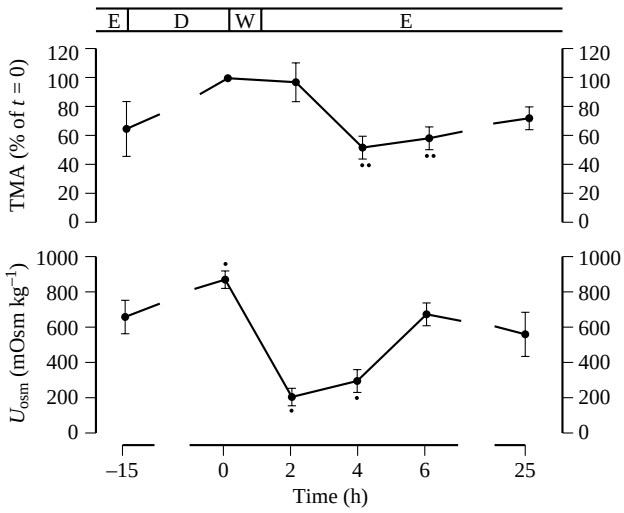

Figure 2 Time-course of changes in medullary TMA levels and U_{osm} in the four volunteers studied. TMA levels are expressed as the TMA area (%) at the point of maximal dehydration (i.e. t = 0). Error bars are ± SEM. $*p < 0.05$ versus t = 0 value for the TMA time-course. $**p < 0.05$ versus $t = -15$ for the U_{osm} time-course. E, euvolemic; D, dehydration; W, water load. (Reproduced by permission of the National Academy of Sciences from Avison et al.[2])

1.2 Phosphorus-31 MRS of Kidney

Jue et al.[3] demonstrated that ^{31}P MRS signals can be obtained from the normal human kidney. Matson et al.[4] also demonstrated the feasibility of obtaining ^{31}P magnetic resonance spectra from human kidneys using the image selected in vivo spectroscopy (ISIS) localization technique. Boska et al.[5] obtained spatially localized ^{31}P magnetic resonance spectra from healthy normal human kidneys and from well functioning renal allographs (Figure 3). Little or no phosphocreatine (PCr) in all spectra verified the absence of muscle contamination and was consistent with proper volume localization. The PME/ATP ratio (PME, phosphomonoester) was slightly elevated in transplanted kidneys (1.1) compared with normal healthy kidneys (0.8). Despite the practical problems produced by organ depth, respiratory movement, and tissue heterogeneity, these results demonstrate the feasibility of obtaining ^{31}P magnetic resonance spectra from human kidneys.

Bretan et al.[6,7] reported their clinical experience with pretransplant assessment of renal viability using ^{31}P MRS to study 40 renal transplant recipient patients (Figure 4). The purpose of their study was to develop and investigate the use of MRS in the clinical transplant setting by correlation of pretransplant MRS parameters with subsequent renal function. Kidneys were studied during simple hypothermic storage within their sterile containers using an external ^{31}P MRS surface coil. Mean storage times were about 38 hours. Cold storage times did not correlate with subsequent clinical renal function. However,

For References see p. 8

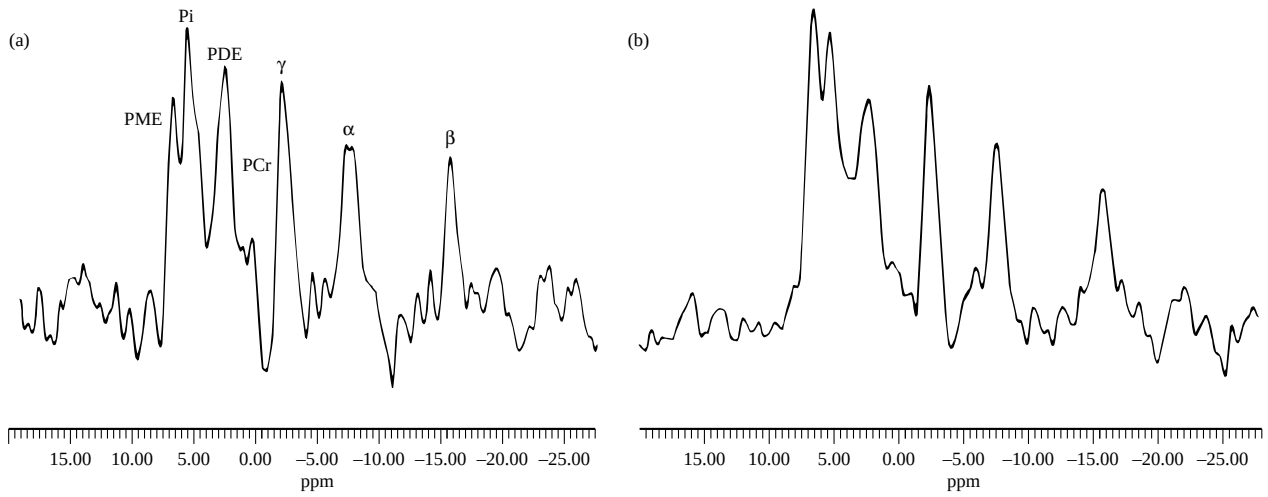

Figure 3 Phosphorus-31 ISIS spectra of (a) the healthy normal kidney and (b) of the well functioning kidney transplant. Acquisition parameters: *TR* = 2.0 seconds, acquisition time = 1 hour, 90° pulse set for the region of interest, distance of the center of the volume of interest (VOI) from the 14 cm surface coil = 70 mm for normal kidney and 42 mm for transplanted kidney, size of the VOI is 25 × 45 × 55 mm = 62 ml for normal kidney and 25 × 50 × 54 mm = 68 ml for transplanted kidney. (Reproduced by permission of Springer-Verlag from Boska et al.[5])

selected ^{31}P MRS data did. ATP was present in 11 kidneys and was associated with the best subsequent renal function. Only 36% of these patients required dialysis, compared with 71 patients without detectable ATP who required a posttransplant dialysis. Kidneys with ATP had the highest PME/Pi (Pi, inorganic phosphate) ratios; in general, the higher the PME/Pi ratio, the better the renal function posttransplant. The intracellular pH did not correlate with subsequent renal function. The authors suggested that MRS provided a better correlation with renal function after transplantation than existing methods.

Grist et al.[8] used ^{31}P MRS to investigate the effects of rejection on renal transplants (Figures 5 and 6). The PDE/PME (PDE, phosphodiester) and Pi/ATP ratios in the transplants with rejection differed significantly from the corresponding metabolite ratios of patients without rejection. A PDE/PME ratio exceeding 0.8 had a sensitivity of 100% and a specificity of 86% for predicting rejection. A Pi/ATP ratio greater that 0.6 had a sensitivity of 72% and a specificity of 86% for predicting rejection. The authors concluded that ^{31}P MRS may be useful as a noninvasive method for evaluating renal metabolism during episodes of transplant rejection.

2 PROSTATE

2.1 Proton MRS of Prostate

Normal prostate has a very high concentration of citrate, a unique feature of this tissue related to the function of prostate cells to secrete citrate into the semen. Most of the MRS of prostate has focused on investigating changes of citrate associated with benign prostatic hypertrophy (BPH) and prostatic carcinoma. Schick et al.[9] investigated the signal characteristics of citrate at low field strengths at 1.5 T using spatially selected spectroscopy and theoretical methods. In vivo localized spectroscopy of small volume elements (2 ml) using a double spin echo method within the prostate gland provided citrate signals. Volume selected proton spectra with different echo times were recorded.

Thomas et al.[10] performed ^{1}H MRS of normal and malignant human prostates in vivo (Figures 7 and 8). The results demonstrated that water-suppressed ^{1}H MRS spectra could be obtained from the prostate. Normal healthy prostate showed a large resonance from citrate. The spectrum from a malignant human prostate showed a much lower level of citrate. The results also suggested that the low concentration of citrate might be useful for the identification of prostate cancer.

Schnall et al.[11] performed localized ^{1}H MRS of the human prostate in vivo using an endorectal surface coil. High levels of citrate were observed in all regions of normal prostate and benign prostatic hypertrophy. The citrate levels in regions containing tumor were variable. The presence of high citrate levels in one case of prostate cancer was confirmed from extracts.

Schiebler et al.[12] reported high-resolution ^{1}H MRS of human prostate perchloric acid extracts (Figure 9). The citrate peak area was higher in benign prostatic hyperplasia than in adenocarcinoma. However, citrate peak areas from the normal peripheral zones were not significantly different from those found in adenocarcinomas. A sharp peak at 2.05 ppm that was seen in four out of thirteen adenocarcinoma samples and only one out of thirteen in the BPH samples was assigned to *N*-acetylneuraminic acid. Fowler et al.[13] also obtained ^{1}H NMR spectra from perchloric extracts of tissue samples from human prostate. Statistically significant differences between the normals, the benign prostratic hypertrophy, and the cancer groups occurred for metabolite ratios of creatine, citrate, and phosphorylcholine. None of the ratios correlated with the Gleason grade of the cancer samples. Different sections of large tumors often yielded substantially different ratios.

Yacoe et al.[14] reported in vitro ^{1}H MRS of normal and abnormal prostate cells (Figure 10).

Proton MRS was used to determine if cell strains derived from prostatic cancers could be distinguished from normal prostate. Prostatic cancer cells had lower concentrations of

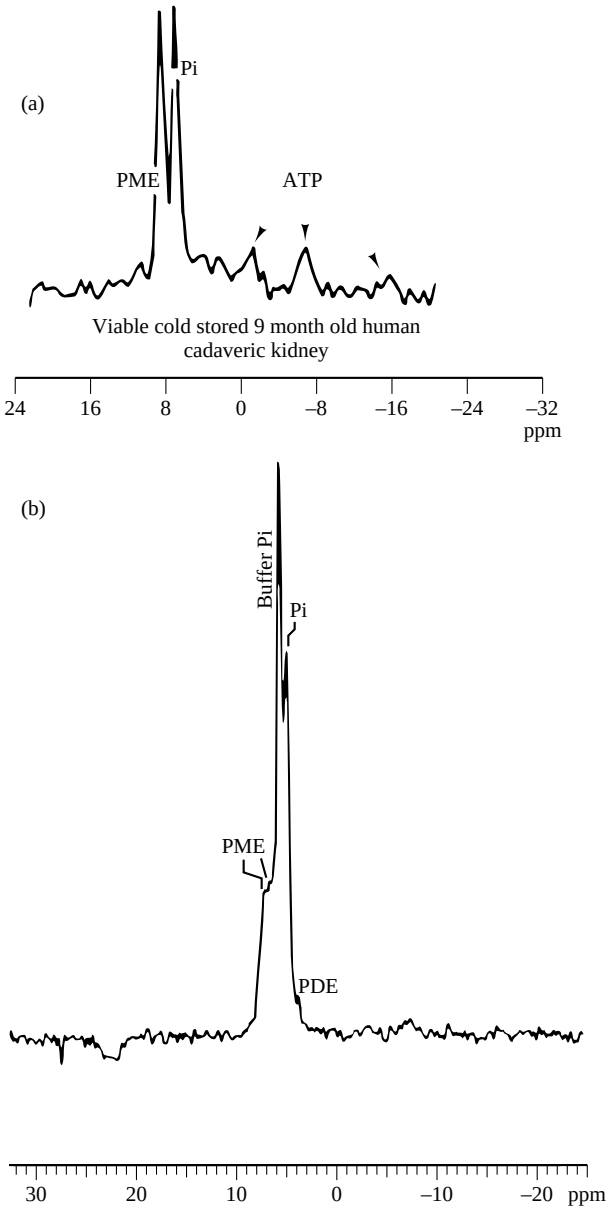

Figure 4 Ex situ in vivo magnetic resonance spectrum of (a) a viable pediatric and (b) an adult kidney. PME, Pi, PDS (phosphodiester), and ATP (adenosine triphosphate) peaks are defined. (Reproduced by permission of Williams & Wilkins from Bretan et al.[6])

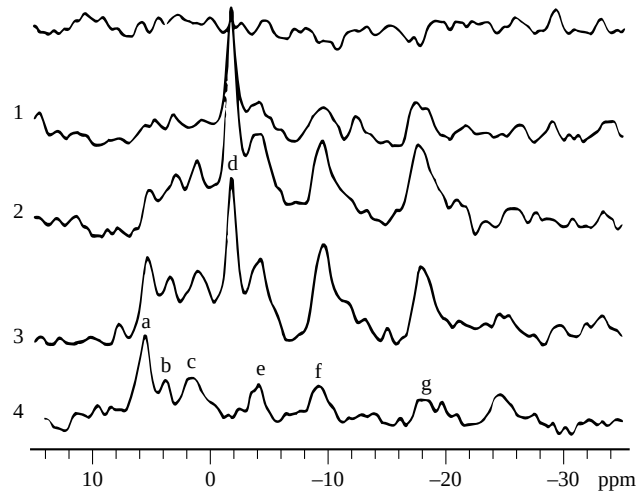

Figure 5 Contiguous ^{31}P magnetic resonance spectra obtained from slices of kidney. Note the presence of significant PCr at the surface, consistent with muscle tissue. The deepest slice shows a large PME peak and little PCr, consistent with renal tissue. Peaks from left to right correspond to PMEs (a), Pi (b), PDEs (c), PCr (d) and γ- (e), α- (f), and β- (g) phosphates of ATP. (Reproduced by permission of Williams & Wilkins from Grist et al.[8])

In the past several years Kurhanewicz, Vigneron and their colleagues have published a series of reports using ^{1}H MRSI of the prostate in a clinical setting. They have used an endorectal coil[16] and a high spatial resolution technique.[17] This

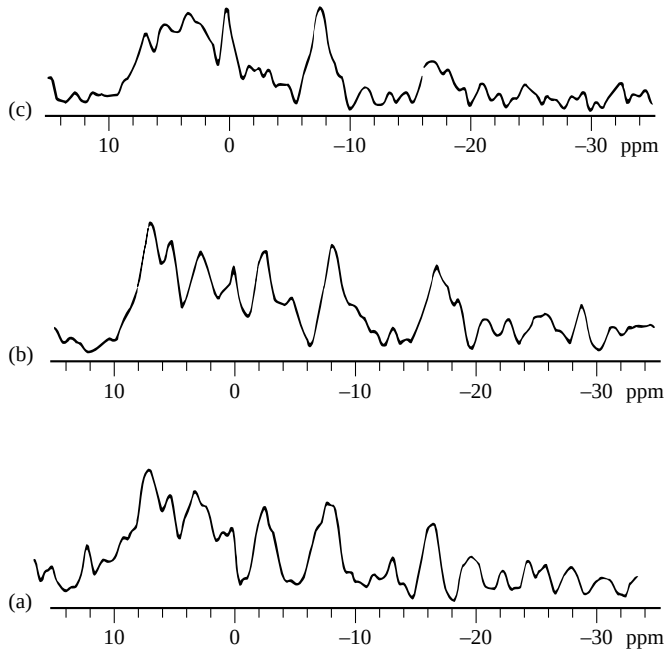

Figure 6 Phosphorus-31 magnetic resonance spectra from a patient with (a) a normally functioning renal allograft, (b) a patient with cyclosporine nephrotoxicity, and (c) a patient with moderate cellular rejection. Note the increase in Pi and PDE in the patient with rejection compared with the normal control subject or the patient with cyclosporine toxicity. PCr is a contaminant from extrarenal tissue. (Reproduced by permission of Williams & Wilkins from Grist et al.[8])

citrate compared with normal prostate epithelium, but the differences were small and not statistically significant. However, both the cancer and normal prostate cells were washed, which may have removed diffusable citrate.

Kurhanewicz et al.[15] performed ^{1}H MRS and enzymatic assays of human prostate adenocarcinomas and prostate DU145 xenographs grown in nude mice. The results showed that citrate concentrations in primary human adenocarcinomas were significantly lower than those observed for normal benign hyperplastic prostatic tissue. There was a 10-fold reduction of citrate associated with DU145 xenographs compared with primary prostate cancer. These findings support the hypothesis that citrate concentrations are low in prostate cancer.

For References see p. 8

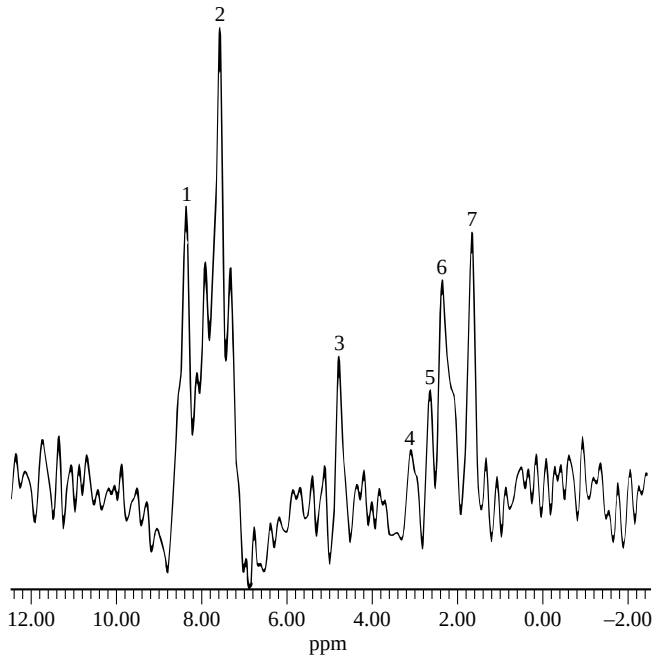

Figure 7 Proton magnetic resonance spectrum prostate in a healthy 26-year-old subject with *TE* = 40 ms. The total acquisition time was 1.5 minutes. Resonance assignments: 1, 2, water and MDPA from the external standard, situated in the plane of the surface coil; 3, residual water; 4, spermine/creatine/PCr; 5, 6, the methylene protons of citrate; 7, methylene protons of spermine and lipids. (Reproduced by permission of the Society for Magnetic Resonance Imaging from Thomas et al.[10])

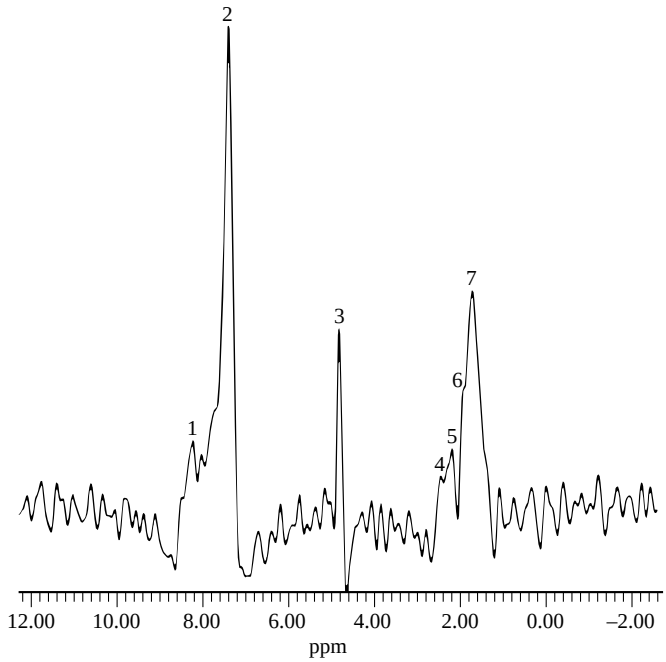

Figure 8 Proton magnetic resonance spectrum of a malignant human prostate with binomial water suppression. Number of scans = 16; repetition time, 5 seconds; *TE* = 80 ms; total acquisition time = 80 seconds. The residual water and the resonances from the external standard were identified at 4.8 and 7.8 ppm, respectively. A 16-step phase cycling was used. Resonance assignments: 1, 2, external standard; 3, residual water; 4, 5, C-2 and C-5 protons of the citrate molecule; 6, 7, methylene protons of spermine and lipids. (Reproduced by permission of the Society for Magnetic Resonance Imaging from Thomas et al.[10])

approach has been used to study the effects of hormone ablation[18] and cryosurgery,[19] and for the detection of local recurrence.[20,21]

2.2 Phosphorus-31 MRS of Prostate

Kurhanewicz et al.[22] reported the use of a ^{31}P MRS transrectal probe for studies of the human prostate (Figures 11–13). The preliminary results indicated that transrectal ^{31}P MRS may characterize ^{31}P metabolites in normal prostates, benign prostatic hyperplastia, and malignant prostates. The preliminary results suggested that malignant prostates are characterized by significantly decreased levels of PCr and increased levels of PME compared to healthy prostates. Thomas et al. evaluated some of the problems encountered with transrectal ^{31}P MRS of human prostate to determine the optimal conditions for these studies.[23] The authors investigated the reproducibility of ^{31}P MRS, regional differences of ^{31}P metabolites, the T_1 relaxation times, and metabolic alterations associated with disease. The PME/ATP ratio was highest in the upper region and lowest in the lower region. Similarly, the PDE/ATP ratio was highest in the upper region and lowest in the lower region. In contrast, the PCr/ATP was lowest in the upper region but was increased in the lower region.

The PME/ATP ratio of normal subjects (0.09 ± 0.1) was increased in the patients with BPH (1.5 ± 0.1) and significantly increased in patients with cancer (1.7 ± 0.2). The PCr/ATP ratio in normal subjects (1.5 ± 0.2) was not significantly reduced in BPH, but it was reduced to 0.9 in prostatic cancer. The PME/PCr ratio in normal subjects was 0.7, was not significantly increased in BPH to 1.4 but was significantly increased in prostate cancer to 2.2.

Hering and Muller reported ^{31}P MRS and ^{1}H MRI of the human prostate with a transrectal probe.[24] Fourteen patients were evaluated with ^{1}H MRI and seven patients with ^{31}P MRS. The PME/ATP ratio was higher in patients with prostatic cancer.

Narayan et al. investigated the ability of ^{31}P MRS to characterize normal human prostate as well as prostate with benign and prosthetic hypertrophy and malignant neoplasms (Figure 14).[25] Normal prostate had PCr/ATP, PME/ATP, and PME/PCr ratios of 1.2, 1.1, and 0.9, respectively. Malignant prostates had PCr/ATP ratios that were lower than normal prostates. Malignant prostates had PME/ATP ratios that were higher than normal prostates.

Using the PME/PCr ratio it was possible to differentiate metabolically malignant prostates from normal prostates with no overlap of individual ratios.

2.3 Carbon-13 MRS of Prostate

Halliday et al. obtained high-quality, high-resolution proton decoupled natural abundance ^{13}C NMR spectra from various human tumors, including prostate (Figure 15).[26]

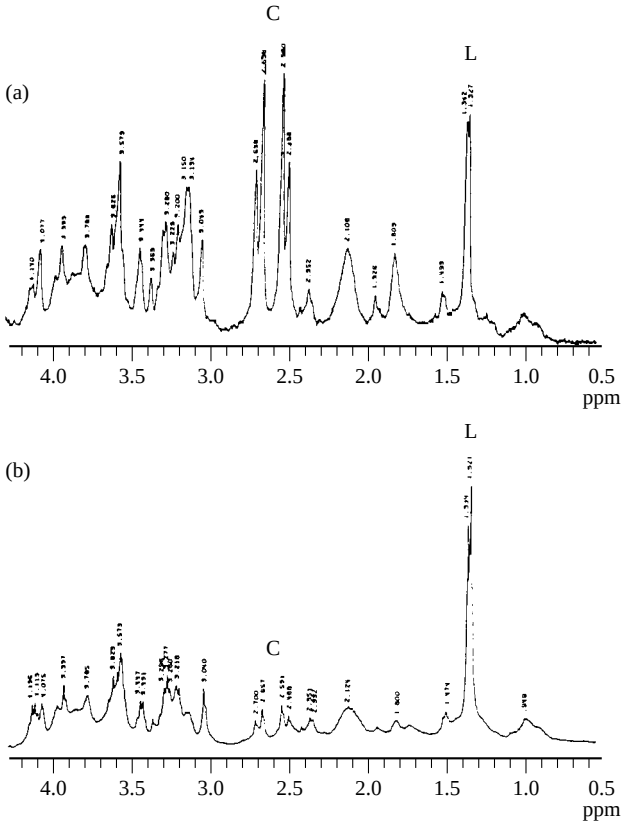

Figure 9 (a) In vitro ^{1}H NMR spectra at 360 MHz, demonstrating a normal pattern with a large citrate peak seen in a sample of benign prostatic hyperplasia with a glandular predominance (C, citrate; L, lactate). Standard not shown. (b) In vitro ^{1}H NMR spectra at 360 MHz for adenocarcinoma showing the expected low citrate peak. Standard not shown. (Reproduced by permission of Williams & Wilkins from Schiebler et al.[12])

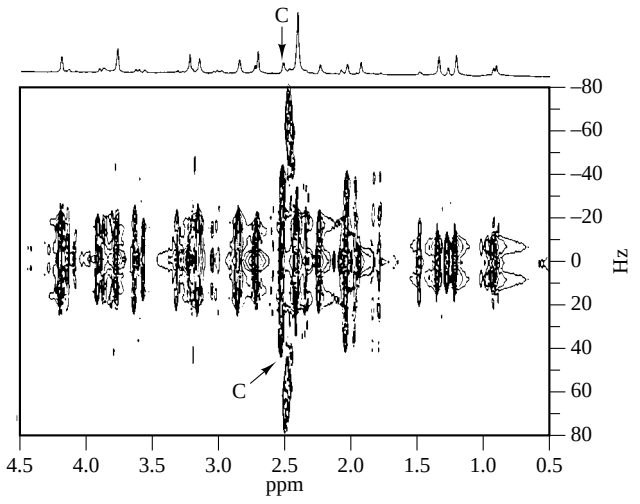

Figure 10 Two-dimensional *J* resolved spectrum of an $HClO_4$ extract of a normal peripheral zone epithelial cell strain, obtained at 500 MHz. The chemical shift is resolved in the horizontal axis and the *J* coupling constant of complex peaks is resolved in the vertical axis. The complex peaks assigned to citrate (C) are pointed out. A one-dimensional projection in the chemical shift dimension is plotted at the top. (Reproduced by permission of Williams & Wilkins from Yacoe et al.[14])

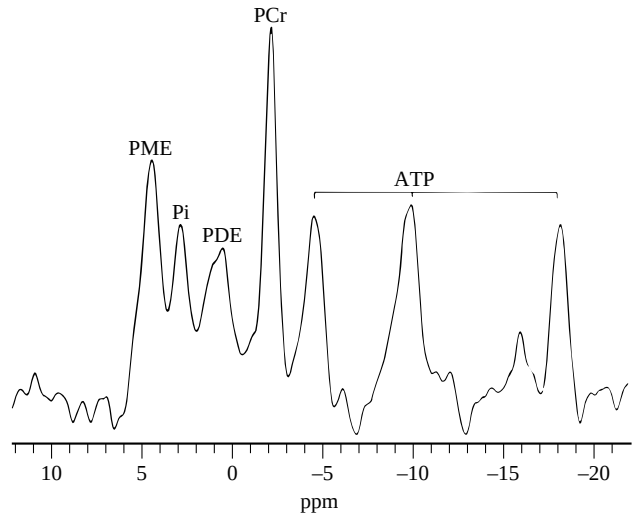

Figure 11 Phosphorus-31 magnetic resonance spectrum of a normal prostate from a normal subject (26 years old), *TR* = 20 seconds; NS = 100. (Reproduced by permission of the Society for Magnetic Resonance Imaging from Thomas et al.[23])

When prostatic adenocarcinoma was compared with adjacent hyperplastic tissue, the tumors were found to contain larger amounts of triacylglycerols, smaller amounts of citrate, and acid mucins. The citrate-to-lipid ratio appeared to differentiate malignant from nonmalignant prostates.[26] Halliday et al. obtained ^{13}C NMR spectra from prostate tumor cell lines.[27] The results showed that the amount of taurine was increased, and tyrosine was decreased in androgen sensitive rat prostatic tumors in comparison to androgen responsive malignant or normal tissue. The authors concluded that the amount of these

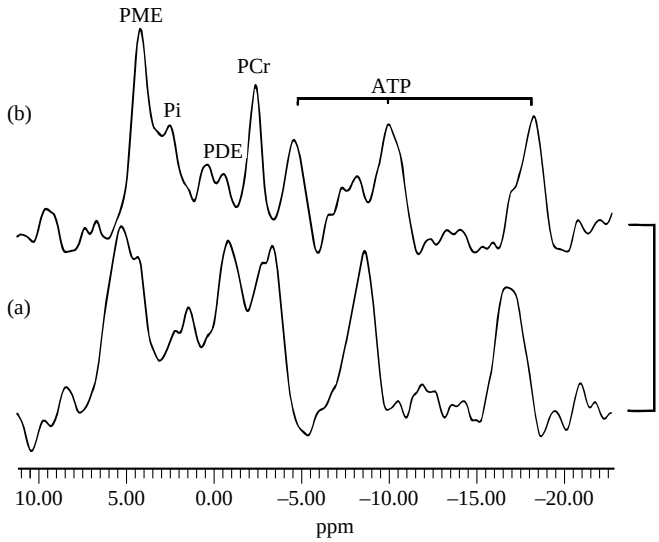

Figure 12 Phosphorus-31 magnetic resonance spectra from human prostates in patients with (a) BPH and (b) prostatic cancer. (Reproduced by permission of the Society for Magnetic Resonance Imaging from Thomas et al.[23])

For References see p. 8

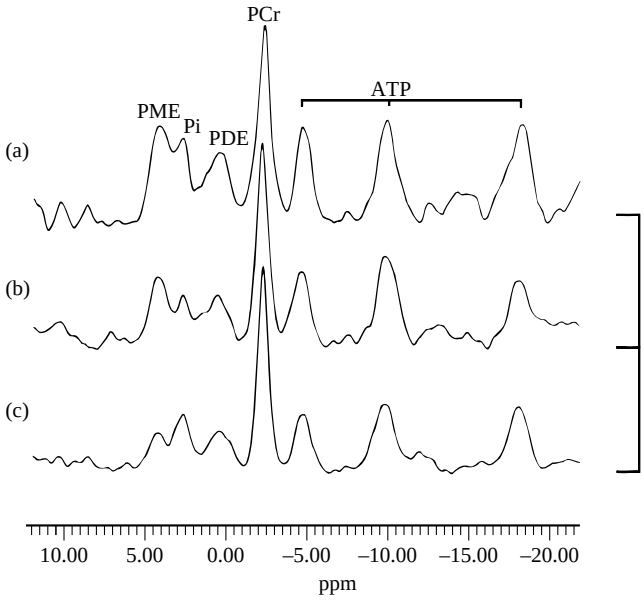

Figure 13 Phosphorus-31 magnetic resonance spectra from (a) upper, (b) middle, and (c) lower regions of the prostate. (Reproduced by permission of the Society for Magnetic Resonance Imaging from Thomas et al.[23])

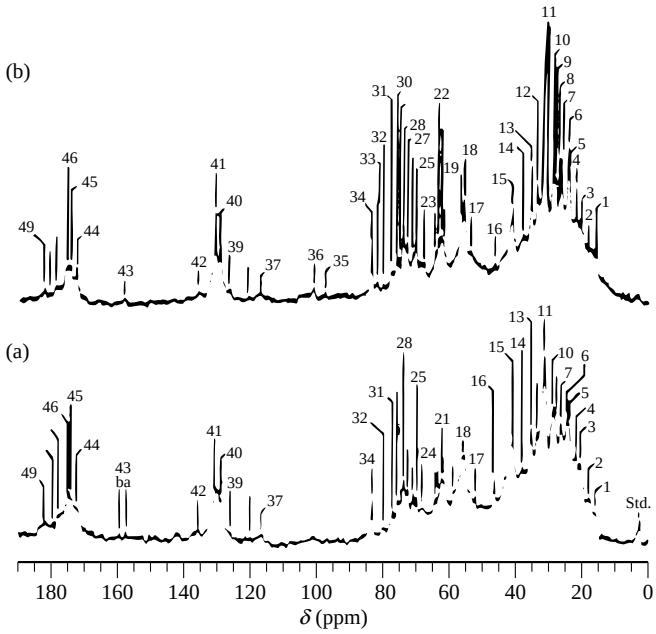

Figure 15 Natural abundance proton decoupled 100.6 MHz ^{13}C NMR spectrum of (a) human prostate with benign prostatic hypertrophy. This proton decoupled spectrum was taken from 2.24 g of tissue, at a temperature of 310 K, with a total of 17 271 scans. (b) A spectrum of poorly differentiated adenocarcinoma of human prostate from the same individual as (a), taken from 3.51 g of tissue with the same parameters, except for the use of 11 241 scans in total. It should be noted that peak 11 is truncated. Assignments for the numbered resonances are given elsewhere.[26] These spectra are representative of seven hyperplastic prostates, three of which contained adenocarcinoma, plus a fourth sample of adenocarcinoma, with the following exception: lactate was increased relative to the control tissue only in the depicted case and resonances from acidic mucins were not present in all of the tumors. (Reproduced by permission of Williams & Wilkins from Halliday et al.[26])

amino acids discriminates androgen-sensitive from insensitive rat prostatic tissues. Sillerud et al. followed this up with an in vivo ^{13}C NMR study of human prostate (Figure 16).[28]

High levels of citrate were measured in the human prostate in vivo as well as the tissue samples of human and rat prostate in vitro.

3 TESTICLE

3.1 Phosphorus-31 MRS of Testicle

Chew et al. investigated the clinical feasibility of ^{31}P MRS to assess the metabolic integrity of the human testicle (Figures 17 and 18).[29] The PME/ATP ratio was greatly reduced in the abnormal testicle; furthermore, the PME/PDE ratio was also reduced in patients with primary testicular failure.

In patients with azoospermia, there were significant differences in the same peak area ratios between patients with primary testicular failure and those with chronic tubular

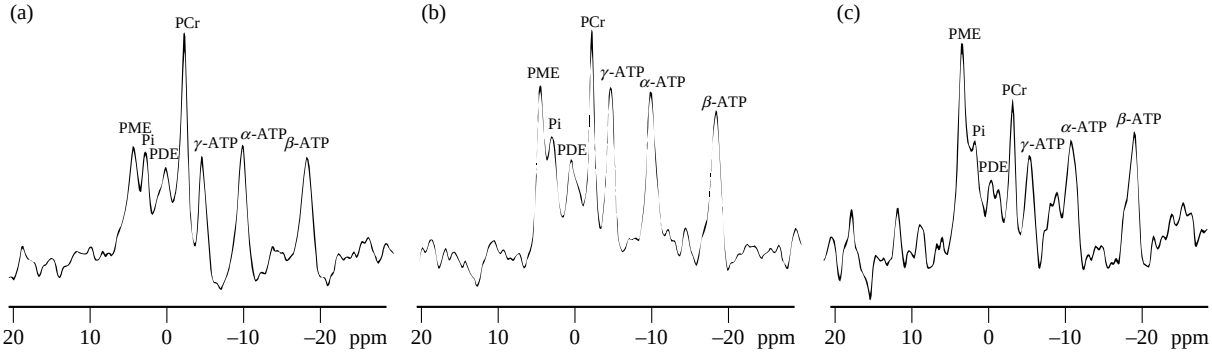

Figure 14 In vivo ^{31}P magnetic resonance prostate spectra. (a) Normal volunteer, (b) patient with BPH, and (c) patient with prostatic cancer. (Reproduced by permission of Williams & Wilkins from Narayan et al.[25])

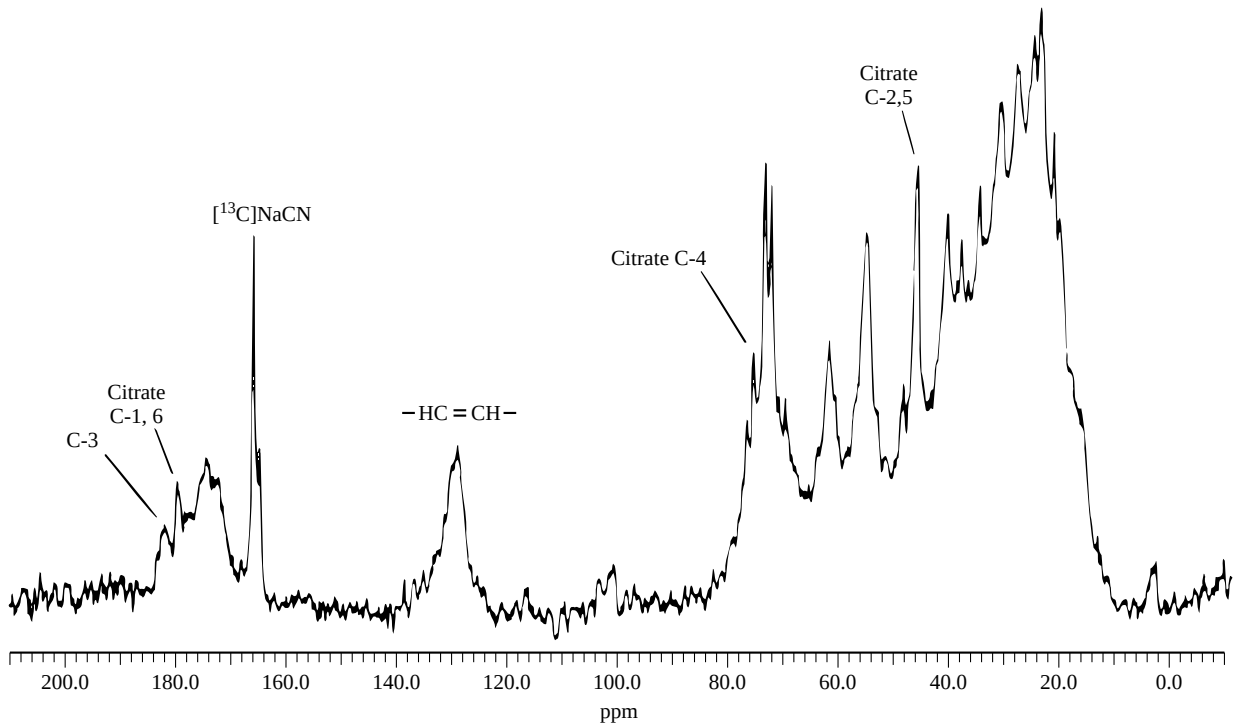

Figure 16 Proton decoupled, natural abundance 100.614 MHz ^{13}C NMR in vitro spectrum from 3.88 g of human benign hypertrophic prostate tissue sample. This spectrum is the average of 13 600 scans at a temperature of 283 K. The signal at 165 ppm is from 15 μl of a 0.15 M [^{13}C]sodium cyanide standard. (Reproduced by permission of Williams & Wilkins from Sillerud et al.[28])

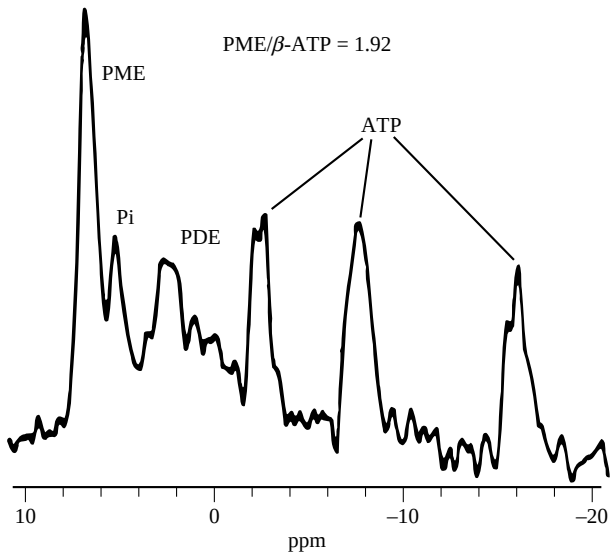

Figure 17 Characteristic ^{31}P magnetic resonance spectrum from the in vivo normal human testicle. Present are the three peaks due to ATP, small signals from PDE and Pi, and a large contribution from the PME peak. This spectrum was acquired with 400 signals averaged in 13.5 minutes. (Reproduced by permission of the Radiological Society of North America from Chew et al.[29])

obstruction. Bretan et al. compared ^{31}P MRS of human testicle with conventional semen analysis.[30] The glycerophosphorylcholine (GPC)/total phosphate ratio in azoospermic men after vasectomy significantly differed from the control GPC/total phosphate ratio, which appropriately reflected complete vasal occlusion. The results suggested that a significant portion of seminal GPC is derived from epidymal secretion and that ^{31}P MRS is useful for monitoring GPC/total phosphate levels when assessing epidymal function in male infertility.

4 UTERUS

High-resolution ^{1}H MRS was used as an adjunct to conventional and histological diagnosis of cervical neoplasia.[31] Cervical biopsy specimens were examined with ^{1}H MRS and the results compared with histology. A high-resolution lipid spectrum was observed in 39 of 40 invasive carcinomas whereas 119 preinvasive samples showed little or no lipids but were characterized by a strong unresolved peak between 3.8 and 4.2 ppm. Peak ratios of the methylene/methyl and the unresolved/methylene resonances allowed accurate distinction between invasive and preinvasive malignancy.

5 RELATED ARTICLES

In Vivo Hepatic MRS of Humans; NMR Spectroscopy of the Human Heart; Proton Decoupling During In Vivo Whole Body Phosphorus MRS; Proton Decoupling in Whole Body Carbon-13 MRS; Quantitation in In Vivo MRS; Whole Body Studies: Impact of MRS.

For References see p. 8

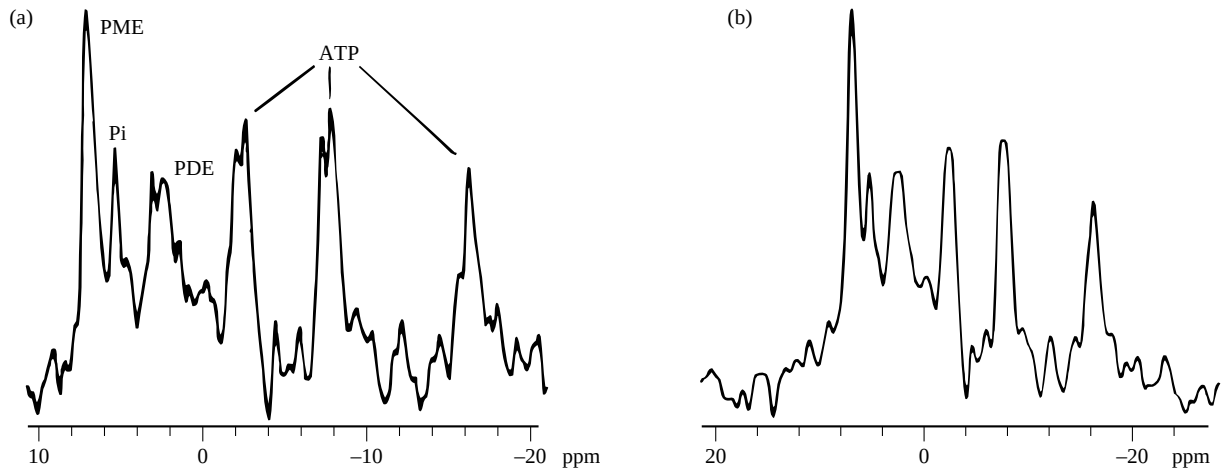

Figure 18 (a) Phosphorus-31 magnetic resonance spectrum from an azoospermic testicle due to primary testicular failure. It is characterized by the same peaks found in the normal spectrum, but the PME/β-ATP peak area ratio is substantially lower (1.32 in this case). (b) Phosphorus-31 magnetic resonance spectrum from an azoospermic testicle due to chronic ductal obstruction. It is characterized by the same peaks found in the normal spectrum, but the PME/β-ATP peak area ratio is lower than normal (1.51 in this case). (Reproduced by permission of the Radiological Society of North America from Chew et al.[29])

6 REFERENCES

1. N. J. Shah, T. A. Carpenter, I. D. Wilkinson, L. D. Hall, A. K. Dixon, C. E. L. Freer, K. Prosser, and D. B. Evans, *Magn. Reson. Med.*, 1991, **20**, 292.
2. M. J. Avison, D. L. Rothman, T. W. Nixon, W. S. Long, and N. J. Siegel, *Proc. Natl. Acad. Sci. USA*, 1991, **88**, 6053.
3. T. Jue, D. L. Rothman, J. A. B. Lohman, E. W. Hughes, C. C. Hanstock, and R. G. Shulman, *Proc. Natl. Acad. Sci. USA*, 1988, **85**, 971.
4. G. B. Matson, D. B. Twieg, G. S. Karczmar, T. J. Lawry, J. R. Gober, M. Valenza, M. D. Boska, and M. W. Weiner, *Radiology*, 1988, **169**, 541.
5. M. D. Boska, D. J. Meyerhoff, D. B. Twieg, G. S. Karczmar, G. B. Matson, and M. W. Weiner, *Kidney Int.*, 1990, **38**, 294.
6. P. N. Bretan, N. Baldwin, A. C. Novick, A. Majors, K. Easley, T. Ng, N. Stowe, P. Rehm, S. B. Streem, and D. R. Steinmuller, *Transplantation*, 1989, **48**, 48.
7. P. N. Bretan, N. Baldwin, A. C. Novick, A. Majors, K. Easley, T. C. Ng, N. Stowe, S. Streem, D. Steinmuller, P. Rehm, and R. Go, *Transplant. Proc.*, 1989, **21**, 1266.
8. T. M. Grist, H. C. Charles, and H. D. Sostman, *Am. J. Roentgenol.*, 1991, **156**, 105.
9. F. Schick, H. Bongers, S. Kurz, W. I. Jung, M. Pfeffer, and O. Lutz, *Magn. Reson. Med.*, 1993, **29**, 38.
10. M. A. Thomas, P. Narayan, J. Kurhanewicz, P. Jajodia, and M. W. Weiner, *J. Magn. Reson.*, 1990, **87**, 610.
11. M. D. Schnall, R. Lenkinski, B. Milestone, and H. Y. Kressel, *Proc. 9th Ann Mtg. Soc. Magn. Reson. Med.*, New York, 1990, p. 288.
12. M. L. Schiebler, K. K. Miyamoto, M. White, S. J. Maygarden, and J. L. Mohler, *Magn. Reson. Med.*, 1993, **29**, 285.
13. A. H. Fowler, A. A. Pappas, J. C. Holder, A. E. Finkbeiner, G. V. Dalrymple, M. S. Mullins, J. R. Sprigg, and R. A. Komoroski, *Magn. Reson. Med.*, 1992, **25**, 140.
14. M. E. Yacoe, G. Sommer, and D. Peehl, *Magn. Reson. Med.*, 1991, **19**, 429.
15. J. Kurhanewicz, R. Dahiya, J. M. Macdonald, L. H. Chang, T. L. James, and P. Narayan, *Magn. Reson. Med.*, 1993, **29**, 149.
16. H. Hricak, S. White, D. Vigneron, J. Kurhanewicz, A. Kosco, D. Levin, J, Weiss, P. Narayan, and P. Carroll, *Radiology*, 1994, **193**, 703.
17. J. Kurhanewicz, D. Vigneron, H. Hricak, P. Carroll, P. Narayan, and S. Nelson, *Radiology*, 1996, **198**, 795.
18. H. Chen, H. Hricak, C. L. Kalbhen, J. Kurhanewicz, D. Vigneron, J. Weiss, and P. Carroll, *Am. J. Roentgenol.*, **166**, 1157.
19. J. Kurhanewicz, H. Hricak, D. B. Vigneron, S. Nelson, F. Parivar, K. Shinohara, and P. R. Carroll, *Radiology*, 1996, **200**, 489.
20. F. Parivar, H. Hricak, J. Kurhanewicz, K. Shinohara, D. B. Vigneron, S. J. Nelson, and P. R. Carroll, *Urology*, 1996, **48**, 594.
21. F. Parivar and J. Kurhanewicz, *Curr. Opin. Urol.*, 1998, **8**, 83.
22. J. Kurhanewicz, A. Thomas, P. Jajodia, M. W. Weiner, T. L. James, D. B. Vigneron, and P. Narayan, *Magn. Reson. Med.*, 1991, **22**, 404.
23. M. A. Thomas, P. Narayan, J. Kurhanewicz, P. Jajodia, T. L. James, and M. W. Weiner, *J. Magn. Reson.*, 1992, **99**, 377.
24. F. Hering and S. Muller, *Urolog. Res.*, 1991, **19**, 349.
25. P. Narayan, P. Jajodia, J. Kurhanewicz, A. Thomas, J. MacDonald, B. Hubesch, M. Hedgcock, C. M. Anderson, T. L. James, E. A. Tanagho, and M. Weiner, *J. Urol.*, 1991, **146**, 66.
26. K. R. Halliday, C. Fenoglio-Preiser, and L. O. Sillerud, *Magn. Reson. Med.*, 1988, **7**, 384.
27. K. R. Halliday, L. O. Sillerud, and D. Mickey, *Proc. 11th Ann Mtg. Soc. Magn. Reson. Med.*, Berlin, 1992, p. 492.
28. L. O. Sillerud, K. R. Halliday, R. H. Griffey, C. Fenoglio-Preiser, and S. Sheppard, *Magn. Reson. Med.*, 1988, **8**, 224.
29. W. M. Chew, H. Hricak, R. D. McClure, and M. F. Wendland, *Radiology*, 1990, **177**, 743.
30. P. N. Bretan, D. B. Vigneron, R. D. McClure, H. Hricak, R. A. Tom, M. Moseley, E. A. Tanagho, and T. L. James, *Urology*, 1989, **33**, 116.
31. E. J. Delikatny, P. Russell, J. C. Hunter, R. Hancock, K. H. Atkinson, C. van Haaften-Day, and C. E. Mountford, *Radiology*, 1993, **188**, 791.

Acknowledgements

Supported by NIH grant R01AG10897 and the DVA Medical Research Service.

For list of General Abbreviations see end-papers

Biographical Sketch

Michael W. Weiner. *b* 1940. B.S., 1961, Johns Hopkins. M.D., 1965, SUNY Upstate Medical Center. Intern and Resident, Mount Sinai Hospital 1965–67. Resident and Fellow in Metabolism, Yale University, 1967–70. Fellow in Biochemistry Institute for Enzyme Research, University of Wisconsin, 1970–72. Faculty at University of Wisconsin, 1971–74, Stanford University, 1974–80, University of California San Francisco, 1980–present. Director, Magnetic Resonance Department, Veterans Affairs Medical Center. Professor of Medicine and Radiology, University of California San Francisco. Research interests include application of MRI to investigation of human metabolism and diagnosis of disease.

For References see p. 8